

¹⁴C DATES AND SPATIAL STATISTICS: MODELING INTRASITE SPATIAL DYNAMICS OF URNFIELD CEMETERIES IN BELGIUM USING CASE STUDY OF DESTELBERGEN CEMETERY

Jeroen De Reu^{1,2} • Guy De Mulder¹ • Mark Van Strydonck³ • Mathieu Boudin³ • Jean Bourgeois¹

ABSTRACT. The possibility of radiocarbon dating on cremated bones stimulated a systematic ¹⁴C dating project investigating the chronology of Late Bronze Age and Early Iron Age urnfield cemeteries in Belgium. The growing amount of ¹⁴C dates on these cremated remains led to new insights into the chronology, development, and disappearance of the urnfield phenomenon. Consequently, ideas about cultural and historical processes need to be modified. Also, the internal chronology of the cemeteries is much more complex than previously thought, stimulating the need for techniques to analyze and visualize the internal development of an individual burial site. The application of centographic methods like the mean center, standard distance circle, and standard deviational ellipse illustrates the possibilities for analyzing the internal chronology of the cemeteries based on the available ¹⁴C dates.

INTRODUCTION

Since the publications of Lanting and Brindley (1998), Lanting et al. (2001), and Lanting and van der Plicht (2001/2002) concerning the possibilities of radiocarbon dating using cremated bones, allowing to date archaeological phenomena that were previously undatable, the number of ¹⁴C-dated cremation remains has grown exponentially. In this light, in the last few years the urnfield cemeteries of the Late Bronze Age and Early Iron Age in Belgium were the subject of a systematic ¹⁴C dating project (De Mulder et al. 2007, 2009; De Mulder 2011), as it was expected that the ¹⁴C dates could shed new light on the chronology and knowledge of the urnfield cemeteries. Traditionally, the chronology of the cemeteries was based on the typochronology of the ceramics, the presence or absence of certain pottery types and/or metals, and the presence of certain types of funerary monuments.

The growing amount of ¹⁴C dates (on cremated bones) led to new insights into the chronological history of these cemeteries, while making clear that ideas and theories about Late Bronze Age and Early Iron Age cultural-historical processes need to be modified (De Mulder 2010). Another resulting observation was that the internal chronology of the individual cemeteries is much more complex than previously thought, which has important consequences for interpreting the internal organization of the burial site. Therefore, this paper aims at discussing, interpreting, and visualizing the genesis, development, and organization of these sites, using the available ¹⁴C dates and intrasite spatial statistics.

The geographic distribution of the cremation graves was measured using a simple spatial centographic analysis method, which uses statistical measures such as the mean and standard deviation and simple geometric forms, including circles and ellipses. A number of distributional characteristics have been calculated for several time intervals based on the ¹⁴C dates. Important parameters are the geographic mean center of the distribution (*mean center*), the clustering or dispersing of graves around this mean center (*standard distance circle*), and the orientation of the distribution (*standard deviational ellipse*). These methods have already been applied and have proven their value in crime analysis (Stephenson 1974; LeBeau 1987; Levine 2006; Kent and Leitner 2007), geography (Jones 1980; Myint 2008; Ayhan and Cubukcu 2010), geology (Mamuse et al. 2009), public health plan-

¹Department of Archaeology, Ghent University, Sint-Pietersnieuwstraat 35, 9000 Ghent, Belgium.

²Corresponding author. Email: Jeroen.DeReu@UGent.be.

³Royal Institute for Cultural Heritage, Jubelpark 1, 1000 Brussels, Belgium.

ning (Tanaka et al. 1981; Khan 1986), and volcanology (Klausen 2004, 2006; Bishop 2007). The application of these centrographic statistics make it possible to track changes in distribution patterns over time, to model movement or to track differences between the distribution patterns of several, different parameters. Despite this, these methods remained rather unexplored in archaeological contexts. To visualize the distribution of graves in time, an interpolation of present/absent graves (per time interval) to a raster surface is made. A preliminary application of this methodology using ^{14}C dates was applied on the Early Mesolithic site of Verrebroek “Dok” (Crombé 2005). At this site, the spatial distribution of the ^{14}C -dated surface hearths was analyzed for unraveling Mesolithic palimpsests (Crombé et al, in press a,b).

In this paper, the ^{14}C dates of the urnfield cemetery of Destelbergen “Eenbeekeinde” (De Laet et al. 1986) are discussed and used for the spatial centrographic analysis to investigate the activities on the cemetery over time.

THE URNFIELD CEMETERY OF DESTELBERGEN

The Traditional Interpretation

The urnfield cemetery of Destelbergen “Eenbeekeinde” is located near the city of Ghent in north-western Belgium (Figure 1). Although the site was discovered in the 1920s during sand extractions, it remained unknown until the end of the 1950s. Subsequently, the site was excavated between 1960 and 1984 under the direction of Professor S De Laet of Ghent University (De Laet et al. 1986). During this period, 105 graves of an urnfield cemetery were uncovered together with a series of funeral monuments (Figure 2), next to a Gallo-Roman settlement that was constructed on top of the urnfield cemetery (De Laet et al. 1985).

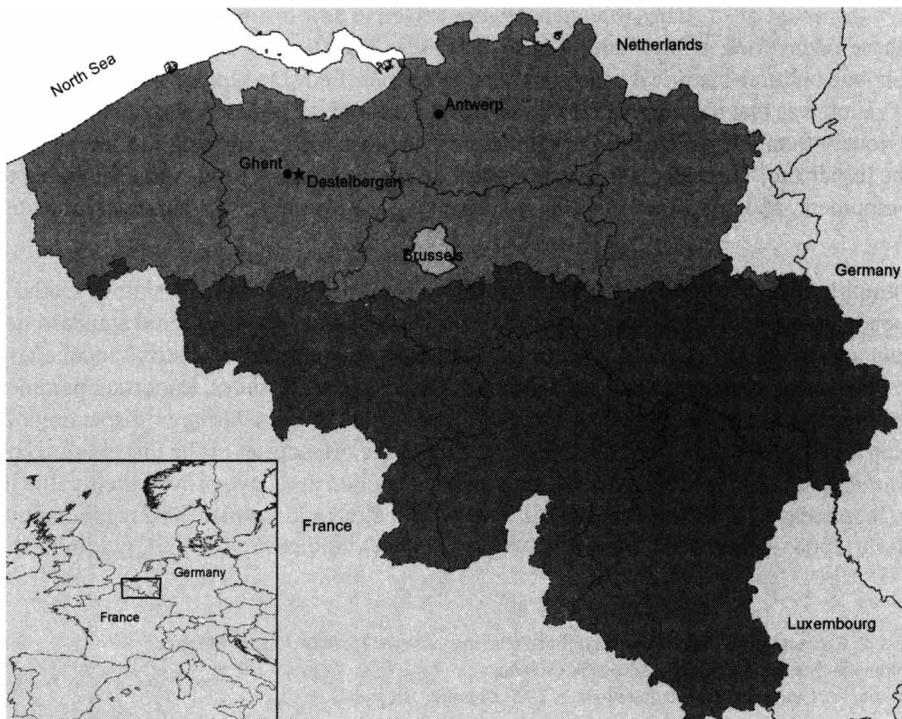


Figure 1 Location of the urnfield cemetery of Destelbergen

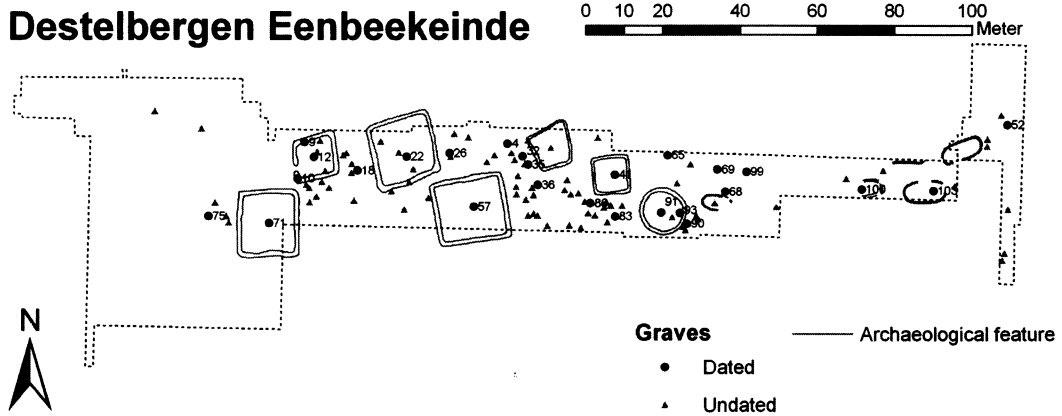


Figure 2 The urnfield cemetery of Destelbergen Eenbeekeinde, with the ¹⁴C-dated graves indicated

The traditional chronology of the site was based on the typo-chronological study of the pottery and the typology of the funeral monuments. According to the traditional interpretation (De Laet et al. 1986; De Mulder 2010), the central grave in the circular monument was interpreted as the founder grave of the burial site (Figure 2). Furthermore, the grave and the associated circular ditched monument (10 m diameter) are situated in the center of the cemetery. It dates to the beginning of the Late Bronze Age (Ha A2, Table 1) as the monument was interpreted in the tradition of the Early and Middle Bronze Age barrows in the region. Where the earlier barrows are much larger (Bourgeois and Cherretté 2005; De Reu et al. 2011a,b), the small size of the monument was an argument to date this monument rather late in or at the end of the Bronze Age barrow tradition. To the east of this barrow, the Late Bronze Age area of the urnfield was located (Figure 2). The graves in this area are associated with ovular structures, interpreted as long barrows (*langbed* in Dutch or *langgrab* in German).

Table 1 The chronological sequence of the Late Bronze Age and Early Iron Age in southern Germany and the neighboring areas based on absolute dates (after Lanting and van der Plicht 2001/2002, 2005/2006).

Chronology	Lanting and van der Plicht (2001/2002)	Calibrated calendar yr	¹⁴ C yr
Middle Bronze Age	Bronzezeit C	1475–1325 BC	3200–3050 BP
Late Bronze Age	Bronzezeit D	1325–1200 BC	3100–3000 BP
	Hallstatt A1 (Ha A1)	1200–1125 BC	3000–2950 BP
	Hallstatt A2 (Ha A2)	1125–1025 BC	2950–2875 BP
	Hallstatt B1 (Ha B1)	1025–925 BC	2875–2800 BP
	Hallstatt B2 (Ha B2)	—	—
	Hallstatt B3 (Ha B3)	925–800 BC	2800–2650 BP
Early Iron Age	Hallstatt C (Ha C)	800–625 BC	2650–2450 BP
	Hallstatt D (Ha D)	625–480 BC	2500–2400 BP
Late Iron Age	La Tène 1	480–250 BC	2450–2200 BP

The area to the west of the round barrow, containing the largest number of graves, was situated in the Early Iron Age. In this zone, 6 quadrangular monuments were excavated (Figure 2). These monuments can be subdivided in 2 groups. One group includes 3 small monuments measuring between 8 and 11 m, while another group includes 3 larger monuments measuring between 16 and 19 m. However, based on the ceramics in their associated central grave, all these monuments were dated

in the Ha C phase (Table 1) of the Early Iron Age. Based on the typo-chronology of the present pottery, characterized by the absence of typical Late Iron Age biconical-shaped ceramics, the urnfield was no longer in use after 450 BC, at the onset of the Late Iron Age.

¹⁴C Dating: Material and Method

The cemetery of Destelbergen Eenbeekeinde has been part of a systematic ¹⁴C dating project investigating the chronology of the Late Bronze Age and Early Iron Age urnfield cemeteries in Belgium (De Mulder et al. 2007, 2009; Van Strydonck et al. 2009, 2010a). At present, 29 cremations have been ¹⁴C dated. Three cremations have been dated only on charcoal (CC), 23 on cremated bone (CB), and the 3 remaining have been double dated on both CC and CB (see also De Mulder et al. 2009). For 2 cremations, the results from the CC and CB matched well (Table 2). The dates from grave 68 match statistically and can be combined according the χ^2 test ($df = 1$, $T = 2.8$ (5% 3.8); R_Combine gr 68: 2837 ± 19 ¹⁴C yr BP). The same positive result has been obtained for grave 75 ($df = 1$, $T = 2.7$ (5% 3.8); R_Combine gr 75: 2455 ± 21 ¹⁴C yr BP). The difference for grave 18 is attributed to an “old wood” effect. On grave 35, a stratigraphical dating analysis has been performed (Van Strydonck et al. 2009). CB samples were treated either using pretreatment with 1% HCl (De Mulder et al. 2007) or with 1N acetic acid (Van Strydonck et al. 2009) to remove secondary carbonate. The first samples were treated according the pretreatment with 1% HCl. After testing, the pretreatment with 1N acetic acid proved to be more efficient in removing possible secondary carbonate. This has been proven by the results on grave 52. A correct date was only obtained using the pretreatment with acetic acid. The pretreatment with 1N HCl delivered a date that was too old according to the archaeological expectation (KIA-37581: 4155 ± 35 BP). For the ¹⁴C dating of the CB, the selection was based on the standards that had already been described (Van Strydonck et al. 2005, 2009, 2010a,b). Only large, thick bones that were cremated at >725 °C were selected. These bones can be recognized by their white color of the surface as well as on the inside.

Table 2 Overview of the ¹⁴C dates on cremated bones (CB) and charcoal (CC) from 3 cremation graves at the urnfield of Destelbergen Eenbeekeinde.

Gr	CB - Lab ID: Date ¹⁴ C yr BP	CC - Lab ID: date ¹⁴ C yr BP
18	KIA-34910: 2330 ± 35	KIA-35797: 2440 ± 30
68	KIA-36925: 2810 ± 25	KIA-34157: 2875 ± 30
75	KIA-34922: 2420 ± 30	KIA-35796: 2490 ± 30

The selection of the samples for this dating project was based on a number of archaeological parameters and research questions, including the typology of the graves and the funeral monuments, the typo-chronological information, and the internal distribution. The 26 graves that were ¹⁴C dated using cremated bone (CB) were used in the spatial analysis of the site (Figure 3, Table 3).

Table 3 Overview of the ¹⁴C dates on cremated bone (CB) from the urnfield of Destelbergen Eenbeekeinde (Gr.: grave ID; A: the weighted average (mean) of the probability density function of the calibrated date (cal BC); B: the median of the probability density function of the calibrated date (cal BC); C: the mode of the probability density function of the calibrated date (cal BC)).

Gr.	Lab ID: date ¹⁴ C yr BP	Cal. date 1σ (BC)	Cal. date 2σ (BC)	A	B	C
69	KIA-37582: 2820 ± 30	1010 (68.2%) 925	1070 (0.3%) 1065 1060 (95.1%) 895	973	972	976
68	KIA-36925: 2810 ± 25	1000 (68.2%) 925	1030 (95.4%) 900	962	961	973
100	KIA-36926: 2785 ± 30	980 (68.2%) 900	1010 (95.4%) 840	935	935	920

Table 3 Overview of the ¹⁴C dates on cremated bone (CB) from the urnfield of Destelbergen Eenbeekeinde (Gr.: grave ID; A: the weighted average (mean) of the probability density function of the calibrated date (cal BC); B: the median of the probability density function of the calibrated date (cal BC); C: the mode of the probability density function of the calibrated date (cal BC)). (Continued)

Gr.	Lab ID: date ¹⁴ C yr BP	Cal. date 1σ (BC)	Cal. date 2σ (BC)	A	B	C
103	KIA-36927: 2775 ± 30	975 (15.7%) 950 945 (42.4%) 890 870 (10.2%) 850	1005 (95.4%) 840	922	921	915
10	KIA-34923: 2755 ± 30	925 (68.2%) 840	980 (95.4%) 825	895	894	904
52	KIA-40553: 2755 ± 30	925 (68.2%) 840	980 (95.4%) 825	895	894	904
99	KIA-36923: 2665 ± 40	895 (7.4%) 875 845 (60.8%) 795	905 (95.4%) 790	837	828	812
26	KIA-35363: 2590 ± 30	805 (68.2%) 770	825 (87.7%) 750 690 (6.3%) 665 615 (1.5%) 595	773	788	794
93	KIA-36922: 2520 ± 30	780 (16.3%) 745 690 (13.5%) 665 645 (29.2%) 585 580 (9.3%) 555	795 (27.6%) 715 695 (67.8%) 535	657	644	672
65	KIA-35364: 2515 ± 30	775 (13.5%) 745 690 (12.9%) 665 645 (47.2%) 550	795 (95.4%) 535	652	640	671
90	KIA-36921: 2505 ± 30	770 (10.5%) 740 690 (10.4%) 660 650 (41.8%) 550	790 (95.4%) 520	644	635	756
35	KIA-comb: 2500 ± 60	775 (19.2%) 705 695 (49.0%) 535	795 (87.4%) 480 470 (8.0%) 415	621	624	626
12	KIA-34892: 2495 ± 30	765 (12.3%) 730 690 (3.7%) 680 675 (4.3%) 660 650 (47.8%) 545	785 (95.4%) 510	636	632	636
36	KIA-30041: 2480 ± 30	760 (17.7%) 705 695 (3.6%) 680 670 (46.9%) 535	770 (90.2%) 500 495 (0.7%) 485 465 (4.5%) 415	623	625	647
41	KIA-37707: 2450 ± 30	745 (21.4%) 685 665 (6.2%) 645 550 (24.3%) 480 470 (16.2%) 415	755 (24.9%) 685 670 (12.7%) 610 600 (57.8%) 405	579	561	537
83	KIA-34893: 2435 ± 35	730 (12.9%) 690 545 (55.3%) 410	755 (20.8%) 685 670 (7.5%) 635 625 (1.2%) 610 600 (66.0%) 400	557	527	516
75	KIA-34922: 2420 ± 30	540 (68.2%) 405	750 (15.6%) 685 670 (4.0%) 640 590 (1.0%) 575 560 (74.9%) 400	525	494	496
22	KIA-37706: 2405 ± 40	540 (68.2%) 400	750 (14.6%) 685 670 (4.1%) 640 595 (76.7%) 390	523	492	411
91	KIA-34179: 2400 ± 30	515 (68.2%) 400	735 (8.3%) 690 665 (1.3%) 650 545 (85.8%) 395	495	474	410
86	KIA-34180: 2390 ± 30	510 (50.8%) 435 425 (17.4%) 400	730 (5.5%) 690 545 (89.9%) 390	482	468	407
32	KIA-35353: 2370 ± 30	505 (28.1%) 460 455 (7.3%) 440 420 (32.9%) 390	705 (0.6%) 695 540 (94.8%) 385	457	448	404
9	KIA-34178: 2360 ± 30	505 (1.2%) 495 490 (16.4%) 460 455 (5.2%) 440 420 (45.3%) 385	525 (95.4%) 380	443	424	402

Table 3 Overview of the ¹⁴C dates on cremated bone (CB) from the urnfield of Destelbergen Eenbeekeinde (Gr.: grave ID; A: the weighted average (mean) of the probability density function of the calibrated date (cal BC); B: the median of the probability density function of the calibrated date (cal BC); C: the mode of the probability density function of the calibrated date (cal BC)). (Continued)

Gr.	Lab ID: date ¹⁴ C yr BP	Cal. date 1σ (BC)	Cal. date 2σ (BC)	A	B	C
18	KIA-34910: 2330 ± 35	415 (68.2%) 365	515 (90.5%) 355 285 (3.9%) 255 245 (0.9%) 235	400	397	397
71	KIA-34887: 2320 ± 30	405 (68.2%) 380	485 (1.1%) 465 420 (87.4%) 355 290 (7.0%) 230	384	393	395
57	KIA-30042: 2215 ± 30	365 (7.3%) 345 320 (27.3%) 270 265 (33.6%) 205	380 (95.4%) 200	283	282	216
4	KIA-34909: 2120 ± 30	200 (68.2%) 100	350 (4.8%) 320 210 (90.6%) 45	150	144	168

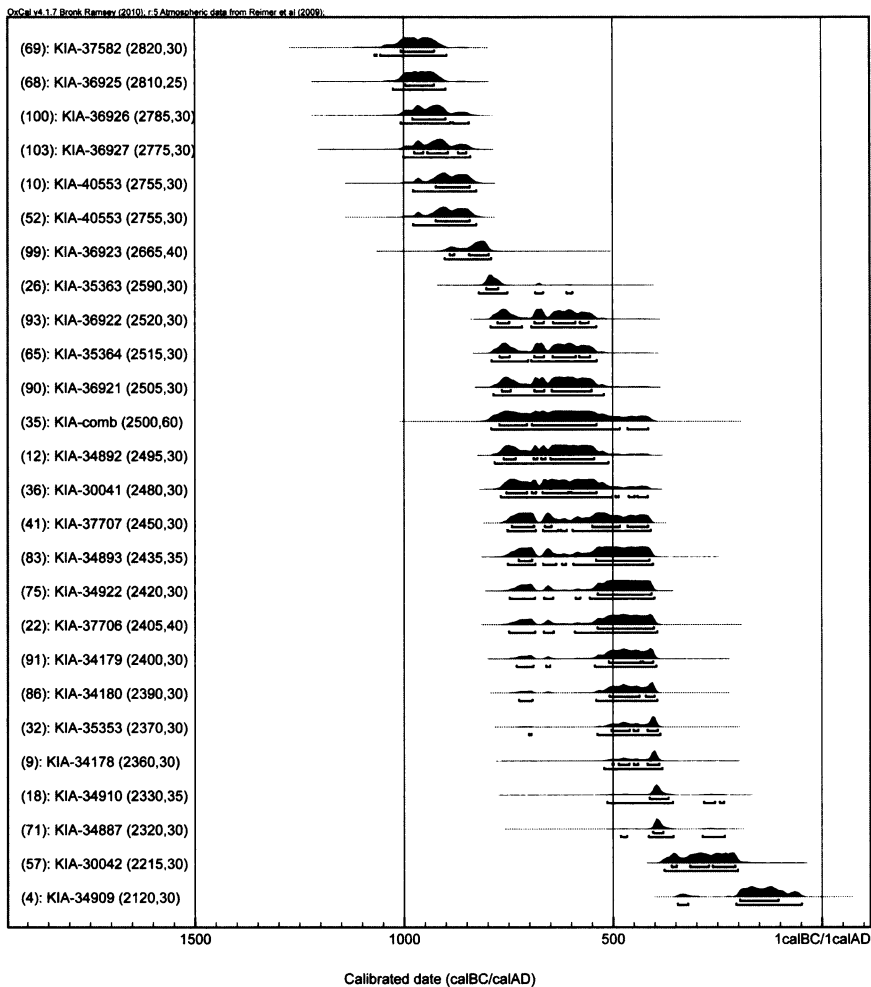


Figure 3 Chronological distribution of the ¹⁴C dates on cremated bone from the urnfield of Destelbergen Eenbeekeinde (OxCal v 4.1.7, Bronk Ramsey 2009; atmospheric data from Reimer et al. 2009).

SPATIAL CENTROGRAPHIC ANALYSIS

Methods for Spatial Centographic Analysis

As mentioned, the spatial centographic analysis method uses statistical measures such as the mean and standard deviation and simple geometric forms, such as circles and ellipses. Three centographic parameters, in particular the *mean center*, *standard distance circle*, and *standard deviation ellipse*, were applied and briefly described here.

The *mean center (MC)* of a point pattern identifies the average (or mean) x and y coordinate or the geographic center (MC) of all distributed points, where

$$MC = (\bar{x}, \bar{y}) = \left(\frac{\sum_{i=1}^n x_i}{n}, \frac{\sum_{i=1}^n y_i}{n} \right)$$

The *standard distance circle (SDC)* represents the standard deviation of the distance (or standard distance) between each point of a point pattern to the mean center (MC) of this point pattern. As such, the standard distance circle measures the degree to which points are distributed around their mean center (MC), where the radius of the circle equals the standard distance (d). The standard distance (d) of the point pattern is given by Levine (2010):

$$d = \sqrt{\frac{\sum_{i=1}^n ((x_i - \bar{x})^2 + (y_i - \bar{y})^2)}{n - 2}}$$

Similar is the *standard deviational ellipse (SDE)*, which measures not only the distribution of geographic points around the mean center (MC) but also the spatial trend or orientation of the distribution. A series of calculations is needed to define the SDE (Lefever 1926; Furfey 1927; Ebdon 1985; Gong 2002; Levine 2010). The rotation angle (θ) of the ellipse is defined as

$$\theta = \arctan \frac{\sum_{i=1}^n (x_i - \bar{x})^2 - \sum_{i=1}^n (y_i - \bar{y})^2 + \sqrt{B}}{2 \sum_{i=1}^n (x_i - \bar{x})(y_i - \bar{y})}$$

where

$$B = (\sum_{i=1}^n (x_i - \bar{x})^2 - \sum_{i=1}^n (y_i - \bar{y})^2)^2 + 4(\sum_{i=1}^n (x_i - \bar{x})(y_i - \bar{y}))^2$$

and the standard deviations for the transposed x axis and y axis are given by

$$SD_x = \sqrt{2 \frac{(\sum_{i=1}^n (x_i - \bar{x}) \cos \theta - \sum_{i=1}^n (y_i - \bar{y}) \sin \theta)^2}{n - 2}}$$

$$SD_y = \sqrt{2 \frac{(\sum_{i=1}^n (x_i - \bar{x}) \sin \theta - \sum_{i=1}^n (y_i - \bar{y}) \cos \theta)^2}{n - 2}}$$

The presented *SDC* and *SDE* formulas are used in Levine's CrimeStat III software (Levine 2006, 2010); however, some other software packages, such as ESRI's ArcGIS, use slightly different formulas. The CrimeStat III software (Levine 2010) was applied for this research.

Centrographic Analysis of the Destelbergen Urnfield Cemetery

Based on the ^{14}C dates, the geographic distribution of the cremation graves was measured by calculating the described spatial distributional characteristics at several time intervals. The geographic location of each grave is defined by the x coordinate and the y coordinate (x, y). The calibrated age was calculated by using the IntCal09 calibration curve (Reimer et al. 2009) and the OxCal 4.1.7 calibration software (Bronk Ramsey 2009). Using the calibrated ^{14}C dates (2σ) of the graves, the *MC*, *SDC*, and *SDE* were calculated for the present graves at 50-yr intervals between 1000 and 350 BC. For example, grave 68 is dated 1030–900 BC (Table 3: KIA-37582). This implies that the grave is used for the calculations of the *MC*, *SDC*, and *SDE* at the time intervals 1000 BC (Figure 4), 950 BC, and 900 BC and not for the time interval between 850 and 350 BC. Another example, grave 9 is dated 525–380 BC (Table 3: KIA-35353), which implies that the grave is used for the calculations at the time intervals 500, 450, and 400 BC (Figure 4) and not for the time intervals 350 BC and between 1050 and 550 BC. Figure 4 illustrates the calculations of the *MC*, *SDC*, and *SDE* for all 26 dated graves, for the time intervals 1000, 800, 600, and 400 BC. Although time, and especially the time range of ^{14}C dates, is difficult to incorporate in a GIS environment (Yuan 2008), an attempt was made to visualize the spatial development of the site in time in a single raster surface (Figure 5). Therefore, point estimates of the calibrated ^{14}C dates were made to obtain a single calibrated year (Telford et al. 2004; Michczyński 2007). Several methods were used to define this "optimal" single year, which can be more easily incorporated in GIS. The first point estimate uses the weighted average (mean) of all age values given by the probability density function of the calibrated date (Table 3, Figure 5). The second option is to derive a date equal to the 50th percentile (or median) of the probability density function of the calibrated date (Table 3, Figure 5). The third calculated date is equal to the date with the highest probability value, or the mode, in the probability density function of the calibrated date (Table 3, Figure 5). Importantly, as stated by Telford et al. (2004) and Michczyński (2007), no single value can adequately describe the complex shape of a ^{14}C probability density function. In this case, the point estimation is forced by the requirements of the applied GIS.

DISCUSSION: ^{14}C DATES AND SPATIAL STATISTICS

Compared to the traditional interpretation of the cemetery, the results of the ^{14}C dating were surprising, indicating that the internal chronology, the occupation, and the development of the site is more complex than previously thought. The first observation is that the cemetery was in use much longer than traditionally expected, ranging between 1070 BC (KIA-37582) and 45 BC (KIA-34909). Seven graves are dated in the Late Bronze Age. The oldest graves (69 and 68), can be situated in the Ha A2–B1 phase (KIA-37582 and -36925). Four graves (100, 103, 10, and 52) can be placed in the Ha B1–B3 phase (KIA-36926, -36927, -34923, and -40553), and 1 grave (99) in the Ha B2–B3 phase (KIA-36923). Except for grave 10, all these Late Bronze Age burials are situated in the eastern sector of the urnfield, where these graves can be associated with the oval funerary monuments (long barrows) (Figures 4, 5). Grave 10 is an urngrave, which had been disturbed and had been deposited in the ditch of a later quadrangular Iron Age monument. The pottery and the cremation remains (charcoal and cremated bone) were deposited in the lower infill of the ditch, which was already silting up at that moment. Grave 12, the central grave of this rectangular monument, has indeed a much younger date (785–510 BC; KIA-34179) than grave 10, indicating the younger date of the monument (Figures 2, 6). The question arises as to why and when this grave has been disturbed. From its

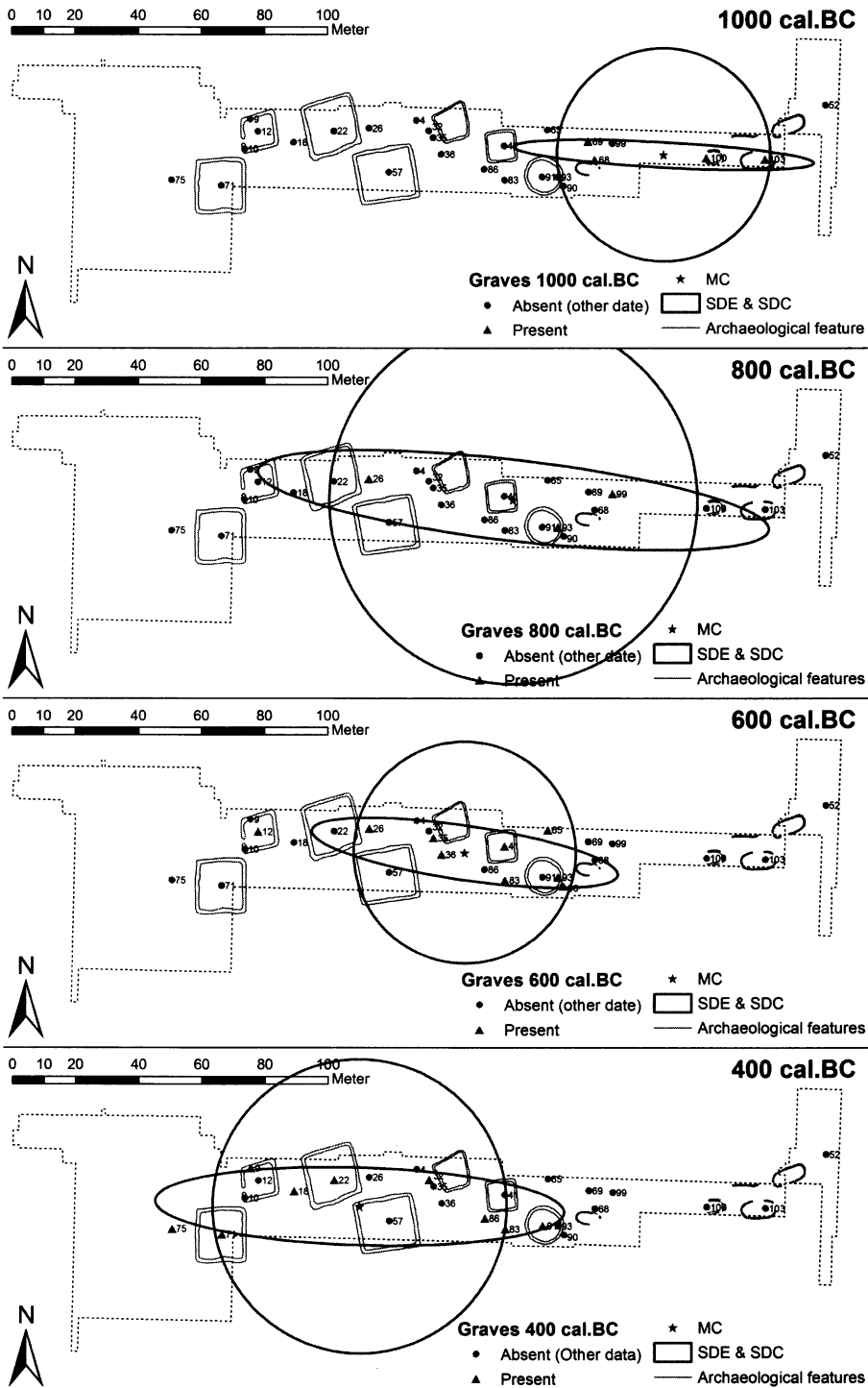


Figure 4 Measuring the activities at the urnfield cemetery at different time intervals, (a) 1000 BC, (b) 800 BC, (c) 600 BC, and (d) 400 BC, using the *MC*, *SDC*, and *SDE* of the present graves.

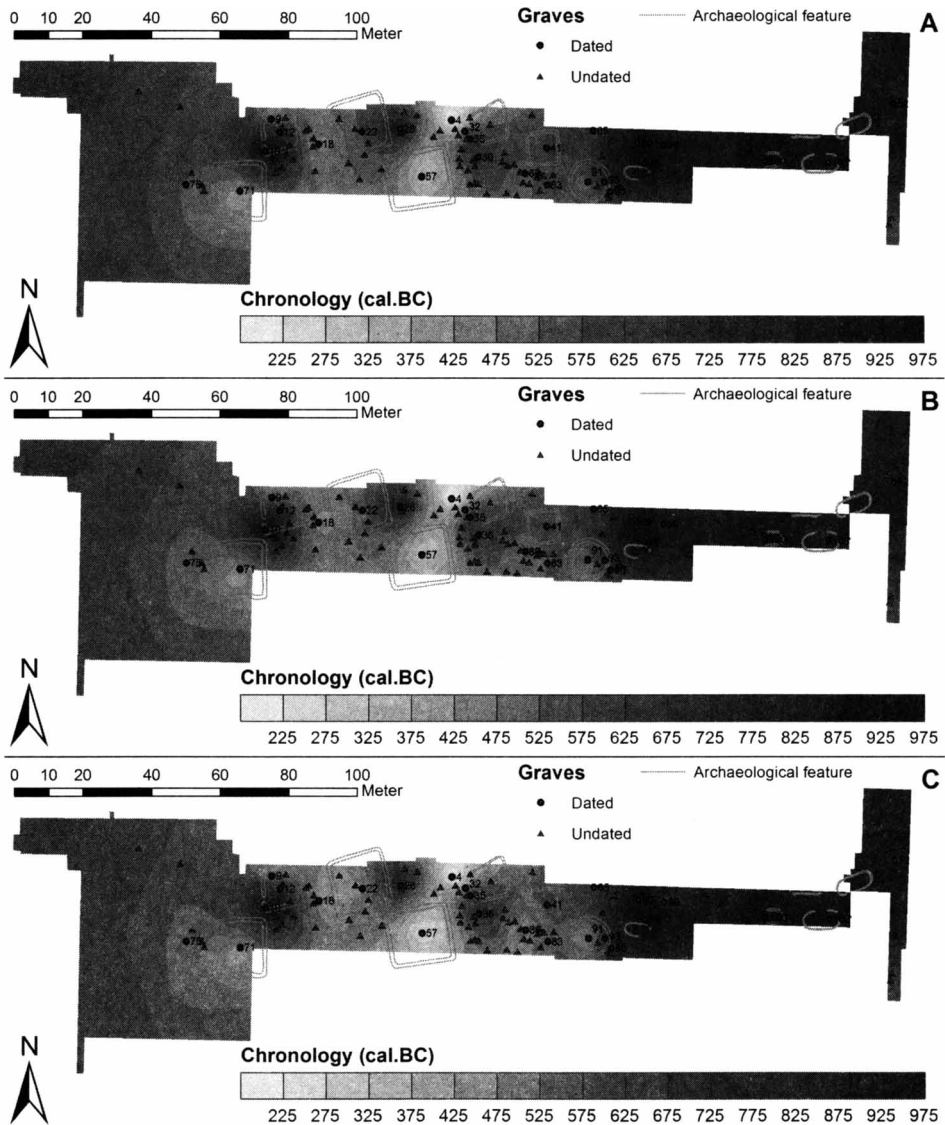


Figure 5 Visualization of the chronological development of the site using A: the weighted average (mean) of the probability density function of the calibrated date; B: the median of the probability density function of the calibrated date; C: the mode of the probability density function of the calibrated date).

stratigraphic position, it is clear that this grave was not unearthed during the erection of the rectangular monument and subsequently reburied in the ditch of the monument. It seems rather that the grave was unearthed at another location in the cemetery, and subsequently deposited in the ditch, which was already filling up. It cannot be excluded that the (re)deposition of the cremation remains in the ditch of the quadrangular monument I was a deliberate ritual reburial. The cremated remains are spread out in an oval shape. Based on the spatial analysis and chronological evolution of the urn-field, it can be suggested that grave 10 was originally located somewhere in the eastern sector of the cemetery and that it was unearthed and reburied during rituals related with the rectangular monument and/or grave 12. In contrast, grave 9 cuts clearly through the infill of the ditch. The ^{14}C date

for this grave is also clearly younger (525–380 BC, KIA-34178) (Figure 6). Although the initial explanation of the excavators is contradictory on this subject, in a first interpretation De Laet et al. (1965) mentioned the digging out of a funeral pit in the filled ditch. Later, this find is interpreted as a deposit during the deliberate filling in of the ditch (De Laet et al. 1986); it is clear that the Late Bronze Age grave 10 has been removed from somewhere in the cemetery and was probably part of a reburial ritual.

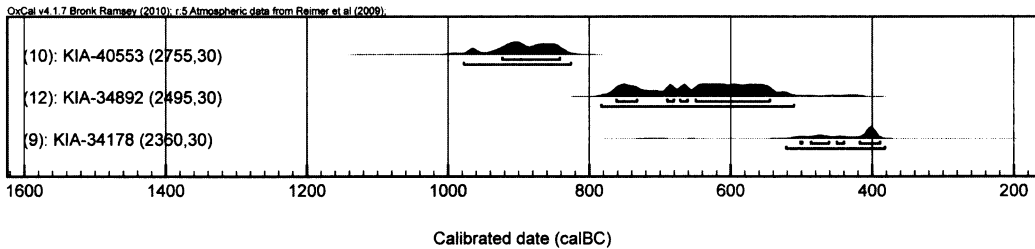


Figure 6 Chronology of the graves associated with the quadrangular monument I (OxCal v4.1.7, Bronk Ramsey 2010; atmospheric data from Reimer et al. 2009).

The majority of the graves are dated to the Early Iron Age; however, the chronology cannot be refined due to the so-called Hallstatt plateau in the ¹⁴C calibration curve. The rectangular monuments already seems to appear from the beginning of the Early Iron Age up into the Late Iron Age, and there is no chronological distinction between the larger and the smaller rectangular monuments. Also, the circular monument seems to be contemporaneous with the rectangular monuments.

The presence of several graves dated to the transitional phase from the Early Iron Age to the Late Iron Age or even completely during the Late Iron Age (Table 3) proves that the cemetery was in use much longer than initially thought based on the typochronology of the pottery (Figures 4, 5). However, the main phase of the cemetery seems to stop at the beginning of the Late Iron Age, ~400 BC (Figure 3, Table 3). Afterwards, the cemetery at Destelbergen was used only sporadically. Only 2 graves (57, 4), or 7.5% of the dated graves, have a younger date than 400 BC (KIA-30042, -34909). The same phenomenon has been attested at 2 other urnfield cemeteries, Kontich and Wijnegem. After the main phase of both cemeteries during the Early Iron Age, some sporadic Late Iron Age cremation graves were also identified by ¹⁴C dating of the cremation remains (De Mulder 2011).

The spatial distribution of the ¹⁴C dates indicates a gradual shift in the activities on the burial site from the eastern sector towards the west. This shift is illustrated by the gradual displacement of the geometric MC of the activities on the cemetery from east to west, which is also supported by the similar displacement of the SDC and SDE (Figure 4). The distinction between the Late Bronze Age and the Early Iron Age part of the cemetery is especially clear (Figure 5). Although the Early Iron Age chronology of the cemetery is less clear due to the Hallstatt plateau, the MC, SDC, and SDE also seem to indicate the shift from east to west. The 2 youngest graves (57 and 4), dated 380–200 BC (KIA-30042) and 350–45 BC (KIA-34909), respectively, are situated in the central part of the Early/Late Iron Age sector of the cemetery (Figure 5) and are as such not fitting in this east-west orientated pattern. As already mentioned, those younger graves seem to represent sporadic reuse during the Late Iron Age, pointing out that these places still had a cosmological meaning associated with funerary practices for the local population. Due to the elongated shape of the excavation, and as a consequence the known elongated distribution pattern of the graves, the SDE produces no significant results, as the outcome of the SDE indicates in all cases an east-west orientation.

In addition, it can be expected that the methodology can be further improved by using weighted *MC*, *SDC*, and *SDE*. In this paper, the *MC*, *SDC*, and *SDE* were calculated for the present graves at each 50-yr time interval between 1000 and 350 BC. A grave is included in the calculations when the 2σ interval of the calibrated ^{14}C date includes the 50-yr time interval for which the centrographic statistics are calculated. However, the probability that the calendar age of a grave is included in the 50-yr time interval differs for the different time intervals. Thus, the inclusion of weights dependent on this probability in the calculations of the *MC*, *SDC*, and *SDE* could possibly further ameliorate the method.

Finally, it is difficult to say which point age estimate of the ^{14}C dates can preferably be used to visualize the spatial development of the cemetery, as there are no large differences in the outcomes of the several point age estimates (Figure 5, Table 3). On average, the range between the minimum and maximum outcome values is 38 yr; however, values of more than 100-yr difference also occur, in particular on ^{14}C dates influenced by the Hallstatt plateau (Table 3). This illustrates again the great difficulty in reducing complex calibrated age distributions into single age points (Telford et al. 2004; Michczyński 2007). Compared to the other two, the point estimate that uses the mode of the probability density function of the calibrated date seems to be the most deviating value (Table 3). Despite this, the output rasters show similar results, all supporting the described trend and interpretation of the cemetery (Figure 5).

CONCLUSION

The systematic ^{14}C dating of urnfield cemeteries has shown that the internal chronology of these burial sites is more complex than previously thought, which has important consequences for the interpretation of the internal organization of these cemeteries. This in turn encourages the need to investigate methodologies for analyzing and visualizing the results of systematic ^{14}C dating on an intrasite level.

Spatial centrographic analysis methods, including the *mean center*, *standard distance circle*, and *standard deviational ellipse*, are used and proved useful to measure the activities on and the development of the cemetery. Calculating these statistics at several time intervals makes it possible to handle the time range of the calibrated dates in a geographic environment (GIS system), where time is difficult to incorporate and to analyze. Interpolation of the ^{14}C dates to raster surfaces proved to be a useful method to visualize the chronology of the site, and as such was an added value to the ^{14}C dates and the interpretation of the site.

ACKNOWLEDGMENTS

The Research Foundation – Flanders (FWO) is thanked for sponsoring the ^{14}C dating project “Funeraire rituelen in het Scheldebekken tijdens de Late Bronstijd en de Vroege IJzertijd (Funerary rituals in the Scheldt basin during the Late Bronze Age and Early Iron Age)” (nr. 1.5.029.07). Our appreciation also goes to Jesper Olsen and Adam Michczyński for their helpful and useful comments and suggestions on the manuscript.

REFERENCES

- Ayhan I, Cubukcu KM. 2010. Explaining historical urban development using the locations of mosques: a GIS/spatial statistics-based approach. *Applied Geography* 30(2):229–38.
- Bishop MA. 2007. Point pattern analysis of eruption points for the Mount Gambier volcanic sub-province: a quantitative geographical approach to the understanding of volcano distribution. *Area* 39(2):230–41.
- Bourgeois J, Cherretté B. 2005. L'âge de Bronze et le premier âge du Fer dans les Flandres Occidentale et Orientale (Belgique): un état de la question. In: Bourgeois J, Talon M, editors. *L'âge du Bronze du nord de la*

- France dans son contexte européen. Actes des congrès nationaux des sociétés historiques et scientifiques, 125^e Lille, 2000. Paris: CTHS. p 43–81.
- Bronk Ramsey C. 2009. Bayesian analysis of radiocarbon dates. *Radiocarbon* 51(1):337–60.
- Crombé P, editor. 2005. *The Last Hunter-Gatherer-Fishermen in Sandy Flanders (NW Belgium). The Verrebroek and Doel Excavation Projects. Volume 1: Palaeo-environment, Chronology and Features*. Ghent: Academia Press. 334 p.
- Crombé P, Sergeant J, Lombaert L, De Reu J. In press, a. The use of radiocarbon dates in unraveling Mesolithic palimpsests: examples from the coversand area of NW Belgium. In: *MESO 2010. The Eighth International Conference in the Mesolithic in Europe* (Santander 13–17 September 2010). Oxford: Oxbow Books.
- Crombé P, Sergeant J, Lombaert L, De Reu J. In press, b. The use of radiocarbon dates in unraveling Mesolithic palimpsests: examples from the coversand area of NW Belgium. In: Souffi B, Valentin B, Ducrocq T, Fagnart J-P, Séara F, Verjux C, editors. *Paletnographie du Mésolithique. Recherches sur les habitats de plain air dans la moitié septentrionale de la France et ses marges*. Actes de la table ronde internationale, 26–27 Novembre 2010, Paris. Paris: Société Préhistorique Française.
- De Laet SJ, Van Doorselaer A, Desittere M, Thoen H. 1965. Verdere opgravingen in het urnenveld te Destelbergen (1965 en 1966). *Oudheidkundige Opgravingen en Vondsten in Oostvlaanderen* 4:10–25.
- De Laet SJ, Thoen H, Bourgeois J. 1985. De opgravingen te Destelbergen/Eenbeekeinde in het raam van de vroegste geschiedenis van de stad Gent I. De voorgeschiedenis. *Handelingen der Maatschappij voor Geschiedenis en Oudheidkunde te Gent, Nieuwe Reeks* 39:3–35.
- De Laet SJ, Thoen H, Bourgeois J. 1986. *Les fouilles du séminaire d'archéologie de la Rijksuniversiteit te Gent à Destelbergen-Eenbeekeinde (1960–1984) et l'histoire la plus ancienne de la région de Gent (Gand). I. La période préhistorique*. Brugge: De Tempel. 225 p.
- De Mulder G. 2010. Old bones, new ideas. ¹⁴C-dating of cremated bones from Late Bronze Age and Early Iron Age urnfield cemeteries in Flanders. In: Sterry M, Tullett A, Ray N, editors. *In Search of the Iron Age*. Proceedings of the Iron Age Research Student Seminar 2008, University of Leicester. School of Archaeology and Ancient History, University of Leicester. p 217–43.
- De Mulder G. 2011. Funeraire rituelen in het Scheldebekken tijdens de late bronstijd en de vroege ijzertijd. De grafvelden in hun maatschappelijke en sociale context [PhD dissertation]. Ghent: Ghent University. 542 p.
- De Mulder G, Van Strydonck M, Boudin M, Leclercq W, Paridaens N, Warmenbol E. 2007. Re-evaluation of the Late Bronze and Early Iron Age chronology of the western Belgian urnfields based on ¹⁴C dating of cremated bones. *Radiocarbon* 49(2):499–514.
- De Mulder G, Van Strydonck M, Boudin M. 2009. The impact of cremated bone dating on the archaeological chronology of the Low Countries. *Radiocarbon* 51(2): 579–600.
- De Reu J, Bats M, Crombé P, Antrop M, Court-Picon M, De Maeyer P, De Smedt P, Finke P, Van Meirvenne M, Verniers J, Werbrouck I, Zwertvaegher A, Bourgeois J. 2011a. Een GIS benadering van de bronstijdgrafheuvel in Zandig-Vlaanderen: enkele voorlopige resultaten (België). *Lumula, Archaeologia Protohistorica* 19:3–8.
- De Reu J, Deweydt E, Crombé P, Bats M, Antrop M, De Maeyer P, De Smedt P, Finke P, Van Meirvenne M, Verniers J, Zwertvaegher A, Bourgeois J. 2011b. Les tombelles de l'âge du bronze en Flandre sablonneuse (nord-ouest de la Belgique): un status quaestionis. *Archäologisches Korrespondenzblatt* 41(4):491–505.
- Ebdon D. 1985. *Statistics in Geography*. 2nd edition. Malden: Blackwell Publishing. 233 p.
- Furley PH. 1927. A note on Lefever's "Standard Deviational Ellipse." *The American Journal of Sociology* 33(1):94–8.
- Gong J. 2002. Clarifying the standard deviation ellipse. *Geographical Analysis* 34(2):155–67.
- Jones BG. 1980. Applications of centrographic techniques to the study of urban phenomena: Atlanta, Georgia 1940–1975. *Economic Geography* 56(3): 201–22.
- Kent J, Leitner M. 2007. Efficacy of standard deviation ellipses in the application of criminal geographic profiling. *Journal of Investigative Psychology and Offender Profiling* 4(3):147–65.
- Khan AA. 1986. Two simple methods of spatial analysis and their applications in location-oriented health services research. *American Journal of Public Health* 76(10):1207–10.
- Klausen MB. 2004. Geometry and mode of emplacement of the Thverartindur cone sheet swarm, SE Iceland. *Journal of Volcanology and Geothermal Research* 138(3–4):185–204.
- Klausen MB. 2006. Geometry and mode of emplacement of dike swarms around the Birnudalstindur igneous centre, SE Iceland. *Journal of Volcanology and Geothermal Research* 151(4):340–56.
- Lanting JN, Brindley AL. 1998. Dating cremated bone: the dawn of a new era. *The Journal of Irish Archaeology* 9:1–7.
- Lanting JN, van der Plicht J. 2001/2002. De ¹⁴C-chronologie van de Nederlandse pre- en protohistorie, IV: bronstijd en vroege ijzertijd. *Palaeohistoria* 43/44: 117–262.
- Lanting JN, van der Plicht J. 2005/2006. De ¹⁴C-chronologie van de Nederlandse pre- en protohistorie, V: midden- en late ijzertijd. *Palaeohistoria* 47/48:241–427.

- Lanting JN, Aerts-Bijma AT, van der Plicht J. 2001. Dating of cremated bones. *Radiocarbon* 43(2A):249–54.
- LeBeau JL. 1987. The methods and measures of centrophography and the spatial dynamics of rape. *Journal of Quantitative Criminology* 3(2):125–41.
- Lefever DW. 1926. Measuring geographic concentration by means of the standard deviational ellipse. *The American Journal of Sociology* 32(1):88–94.
- Levine N. 2006. Crime mapping and the Crimestat program. *Geographical Analysis* 38(1):41–56.
- Levine N. 2010. CrimeStat III: a spatial statistics program for the analysis of crime incident locations (version 3.3). Houston/Washington DC: Ned Levine & Associates & National Institute of Justice.
- Mamuse A, Porwal A, Kreuzer O, Beresford S. 2009. A new method for spatial centrophographic analysis of mineral deposit clusters. *Ore Geology Reviews* 36(4):293–305.
- Michczyński A. 2007. Is it possible to find a good point estimate of a calibrated radiocarbon date? *Radiocarbon* 49(2):393–401.
- Myint SW. 2008. An exploration of spatial dispersion, pattern, and association of socio-economic functional units in an urban system. *Applied Geography* 28(3):168–88.
- Reimer PJ, Baillie MGL, Bard E, Bayliss A, Beck JW, Blackwell PG, Bronk Ramsey C, Buck CE, Burr GS, Edwards RL, Friedrich M, Grootes PM, Guilderson TP, Hajdas I, Heaton TJ, Hogg AG, Hughen KA, Kaiser KF, Kromer B, McCormac FG, Manning SW, Reimer RW, Richards DA, Southon JR, Talamo S, Turney CSM, van der Plicht J, Weyhenmeyer CE. 2009. IntCal09 and Marine09 radiocarbon age calibration curves, 0–50,000 years cal BP. *Radiocarbon* 51(4):1111–50.
- Stephenson LK. 1974. Spatial dispersion of intra-urban juvenile delinquency. *Journal of Geography* 73(3):20–6.
- Tanaka T, Ryu S, Nishigaki M, Hashimoto M. 1981. Methodological approaches on medical care planning from the viewpoint of geographical allocation model: A case study on South Tama district. *Social Science & Medicine. Part D: Medical Geography* 15(1):83–91.
- Telford RJ, Heegaard E, Birks HJB. 2004. The intercept is a poor estimate of a calibrated radiocarbon age. *The Holocene* 14(2):296–8.
- Van Strydonck M, Boudin M, Hoefkens M, De Mulder G. 2005. ¹⁴C-dating of cremated bones, why does it work? *Lunula, Archaeologia Protohistorica* 13:3–10.
- Van Strydonck M, Boudin M, De Mulder G. 2009. ¹⁴C dating of cremated bones: the issue of sample contamination. *Radiocarbon* 51(2):553–68.
- Van Strydonck M, Boudin M, De Mulder G. 2010a. The carbon origin of structural carbonate in bone apatite of cremated bones. *Radiocarbon* 52(2–3):578–86.
- Van Strydonck M, Boudin M, De Mulder G. 2010b. Een status quaestionis van ¹⁴C-dateringen op gecremeerd bot. *Lunula, Archaeologia Protohistorica* 18:5–12.
- Yuan M. 2008. Adding time into geographic information system databases. In: Wilson JP, Fotheringham AS, editors. *The Handbook of Geographic Information Science*. Malden: Blackwell Publishing. p 169–84.